Submitted to Phys. Rev. A

LBL-2148
Preprint

c.1

DE-EXCITATION RATES FOR $He^+(2S)$ IN COLLISION WITH ATOMS AND MOLECULES

M. H. Prior and E. C. Wang

October 25, 1973

Prepared for the U.S. Atomic Energy Commission
under Contract W-7405-ENG-48

For Reference

Not to be taken from this room

LAWRENCE BERKELEY LABORATORY
UNIVERSITY OF CALIFORNIA
BERKELEY

c.1

LBL-2148

DISCLAIMER

This document was prepared as an account of work sponsored by the United States Government. While this document is believed to contain correct information, neither the United States Government nor any agency thereof, nor the Regents of the University of California, nor any of their employees, makes any warranty, express or implied, or assumes any legal responsibility for the accuracy, completeness, or usefulness of any information, apparatus, product, or process disclosed, or represents that its use would not infringe privately owned rights. Reference herein to any specific commercial product, process, or service by its trade name, trademark, manufacturer, or otherwise, does not necessarily constitute or imply its endorsement, recommendation, or favoring by the United States Government or any agency thereof, or the Regents of the University of California. The views and opinions of authors expressed herein do not necessarily state or reflect those of the United States Government or any agency thereof or the Regents of the University of California.

LBL-2148

De-excitation Rates for $He^+(2S)$ in Collision with Atoms and Molecules.†

M. H. Prior and E. C. Wang

Department of Physics and Lawrence Berkeley Laboratory
University of California, Berkeley, California 94720

ABSTRACT

We have studied the de-excitation of He^+ ions in the 2S metastable state by collision with eleven different target gases. These include noble gases, symmetric linear molecules, water and ammonia. From our data we extract velocity averaged total de-excitation rate constants, $\langle \sigma v \rangle$, ranging from $1.65(17) \times 10^{-9}$ to $20.9(21) \times 10^{-9}$ cm^3 sec^{-1} for helium and ammonia, respectively. In all cases the mean energy of the He^+ ions was $\simeq$ .44 eV and the target gases had a 300°K Maxwell-Boltzmann distribution of velocities. The results are consistent with collision induced Lyman-α emission being a prominent de-excitation mechanism.

I. Introduction

In the past a fair amount of experimental and theoretical effort has been expended on the problem of the de-excitation of hydrogen atoms in the metastable 2S state by near thermal energy collisions with atoms and molecules. Both experimentally and theoretically the problem seems to be tractable, a circumstance which adds the usual synergistic term to the rate of progress. Most recently there has been the experimental work of Kass and Williams,[1] Czuchlewski and Ryan[2], and Comes and Wenning.[3] Preceding these was the pioneering work of Fite[4,5] and collaborators. On the theoretical side recent papers by Byron[6] and Gersten[6,7] and Slocomb, Miller and Schaeffer[8] are notable.

In this work we report experimental studies of the nearly analogous problem of collisional de-excitation of $He^+(2S)$. Exact analogy fails because the positive charge of the ion plays an important role, but the broad picture of the de-excitation process remains.

Briefly, the current understanding is that the transient electric field seen by the metastable projectile during its passage near a target atom or molecule mixes the 2S and 2P states via the Stark interaction, leaving it with a finite probability of being in one of the 2P states after the collision. Since the lifetime of the 2P state is very short ($\simeq 10^{-9}$ sec for H, 10^{-10} sec for He^+), the projectile returns to the ground (1S) state emitting a Lyman-α photon ($\lambda \simeq 300$Å for He^+) long before it can meet another target.

The interaction potential responsible for the transient field will depend, of course, upon the nature of the target and the charge of the hydrogen-like metastable projectile. In the case of H(2S) in collision with a spherical target (e.g. a noble gas atom) the interaction is, roughly,[8] that of the transient (2S + 2P) quadrupole moment interacting with the electric field produced by the dipole induced in the target by the (2S + 2P) dipole moment. Thus it is proportional to the polarizability of the target and has a r^{-7} dependence on the separation r. In the case of molecular collisions the interaction is generally of longer range being via the electric multipole field surrounding the target. Thus for polar molecules the interaction potential is proportional to the molecular dipole moment and falls as r^{-3}. When the metastable projectile is charged, as with $He^+(2S)$, one has in addition to consider the interaction induced by the Coulomb field. This yields a potential proportional to the target dipole polarizability and varying as r^{-4}.

The de-excitation rates measured in this work are total rates; i.e. they are the sum of the rates for all processes leading to de-excitation of $He^+(2S)$. Since $He^+(2S)$ possesses 40.8 eV of excitation energy, a host of de-excitation mechanisms are possible. The most probable are induced Lyman-α decay as described above and non-radiative de-excitation with simultaneous ionization of the target (Penning ionization); i.e. the process,

$$He^+(2S) + X \rightarrow He^+(1S) + X^+ + e^- .$$

In addition when the target is a molecule, a number of ion-neutral reactions are possible. Many of these would lead to dissociation and ionization of the target molecule. Very little, if any, information is available for rates of such processes when the projectile is a highly excited metastable ion such as $He^+(2S)$. We believe, however, that regardless of the target, the induced Lyman-α rate accounts for more than half of the total de-excitation rate. We present some experimental evidence which shows that for collisions with He, it is a prominent process.

II. Experimental Method

The present work is an outgrowth of an experiment[9] carried out to measure the free lifetime, τ_0, of $He^+(2S)$. The result of that experiment was $\tau_0 = 1.922(82)$ msec. which is in agreement with the theoretical value[10] of 1.899 msec. The same apparatus was used in these experiments with some modefications, principally to allow absolute measurement of target gas pressure increments.

The unperturbed 2S state decays by emission of two electric dipole photons[11] with energies such that $h\nu_1 + h\nu_2 = 40.8$ eV. The single photon distribution is then a continuous one with a short wavelength cutoff at $\lambda_{min} = 304$ Å and extending to infinite wavelength.

The distribution[12] rises rapidly from λ_{min} to a peak at $\simeq$ 350Å after which the intensity falls off roughly as $\exp[-(\lambda-350)/430]$.

The method used is based on the following simple ideas. If one has a quantity N of $He^+(2S)$ ions confined to some volume containing a density n_{He} of helium atoms and n of target atoms or molecules then the usual simple first order differential equation applies to the variation of N with time;

$$dN/dt = -N(A+\sigma_{He}vn_{He}+\sigma vn) \qquad (1)$$

where $A = 1/\tau_0$, σ_{He} and σ are total de-excitation cross-sections for collisions with helium and the target of study; v is the relative collision velocity (here assumed to be the same for each type of collision). The solution is

$$N = N(t=0)e^{-t/\tau}, \qquad (2)$$

where

$$1/\tau = A+\sigma_{He}vn_{He}+\sigma vn \qquad (3)$$

Thus, if one holds v and n_{He} constant, a plot of the measured quantities $1/\tau$ vs. n should yield a straight line whose slope is the product σv. If one has a unique and known value of v then one could extract σ. In these experiments, however, one has present a distribution of relative velocities so that the quantity derived from such a plot is $R = \langle \sigma v \rangle$, the velocity averaged product. It turns out that the distribution of v present in the measurements reported here is, to a good approximation, independent of the target, and hence trends in R reflect trends in σ.

The technique used to measure $1/\tau$ vs n is as follows. A quantity ($\simeq 10^2$) of $He^+(2S)$ ions are created by pulsed electron impact on He gas ($p_{He} \approx 10^{-6}$ Torr) at time t = 0. The ions are confined inside an electromagnetic ion trap for a period of 4 msec. During this storage time the $He^+(2S)$ ions make collisions with the He gas and with the target gas at a pressure p; single decay photons are detected by windowless electron multipliers and the resulting pulses are stored versus time in 100 channels of a multichannel scalar (40 μsec/channel). At the end of the storage period, all ions are dumped from the trap and a new cycle is begun. Many fill-store-dump cycles are repeated until a decay curve is accumulated with sufficiently small statistical fluctuations to allow determination of a value for τ. This may take from 15 minutes to 2 hours depending on the experimental conditions. The whole process is repeated for different values of p to determine the line $1/\tau$ vs n ($n = p/kT$).

Figure 1 shows the ion trap and photon detectors. The ion trap is a closed cylinder (radius $\simeq$ 15 cm, length $\simeq$ 30 cm) whose ends are maintained at a positive potential with respect to the body; the potential difference during these measurements was 2.0 volts. A magnetic field of $\simeq$ 60 gauss was applied coaxial with the cylinder by means of coils external to the vacuum enclosure. The electrostatic field confines ion motion along the magnetic field, while the magnetic field limits motion perpendicular to the trap axis.

The trap is constructed primarily from oxygen-free high-conductivity copper, stainless steel, and alumina insulators; the vacuum enclosure is entirely of stainless steel. After bake-out pressures of $<2 \times 10^{-9}$ Torr have been achieved, however during these measurements the background pressure was more typically $\simeq 8 \times 10^{-8}$ Torr. Helium and target gases are admitted to the chamber containing the trap via separate micrometer controlled variable leak valves. These in turn are connected to separate gas handling systems. The micrometer valves allowed sensitive control of p_{He} and p during the measurements. A quadrupole residual gas analyzer is attached to the chamber and is used to monitor the constituents of the background gas and the purity of the admitted target gas.

Helium ions are created inside the trap by impact from an electron pulse accelerated along the axis. Typically the electron pulse is 4.0 μA, last 0.75 msec, and has an energy of 225 eV. At a helium pressure of 8×10^{-6} Torr this yields about 10^6 ions, of which about 10^3 can be expected to be in the 2S metastable state. At the end of a storage period the trap potentials are altered so that ions are dumped onto a collecting plate (electrode 4 in Fig.1); this allows monitoring of the number of stored ions via the size of the resulting positive current pulse which was displayed on an oscilloscope and averaged via a boxcar integrator. The electron pulse also appears on this electrode during the trap fill time. Of course, background and target gas ions are created by the electron pulse in addition to He ions, However, except for the case when the target gas is H_2,

these ions have too small a charge to mass ratio to be confined and in a fraction of a millisecond leave the trap volume - - only the He ions remain. The heavy ions do compete for space in the trap, however, during the fill period and the transient period during which they leak from the trap, and, since the trap has a finite capacity for confined charge ($\approx 10^7$ positive charges), they affect the number of He ions which are ultimately stored for a given electron pulse. One observes a decrease in the number of stored He ions when one holds the electron pulse and p_{He} constant and increases p. This effect is one of the factors limiting the range over which p may be varied for a given target.

As is indicated in Fig.1, the cylindrical portion of the trap is made up of two half cylinders 2a and 2b; this allows application of an alternating potential between them (while maintaining a common dc potential) which can excite resonant motion of the stored ions at their cyclotron frequency. At resonance the ions gain energy from the ac field until they strike the electrodes or chamber walls; thus one observes a drop in the ion dump-pulse amplitude when the applied frequency is in resonance. In addition to the cyclotron resonance, one observes resonance at the frequency of motion along the trap axis (z-motion) and at the magnetron frequency (frequency of drift of the cyclotron orbit center about the trap axis). To excite the z-motion resonance it is more convenient to apply the ac potential between electrodes 1 and 2a, 2b connected together.

Observation of the z-motion resonance allows determination of

the effective harmonic potential well depth, W, along the z-axis. Thus $W = kz_m^2/2q$ where $k = m(2\pi f_z)^2$ and z_m is the maximum amplitude of z-motion, q the ion's charge, m it's mass, and f_z the z-motion frequency. For helium ions with trap potentials as described above, f_z was measured to be $f_z = 7.98(50)$ kHz. With $z_m = 12.9$ cm one obtains $W = .87(11)$ eV.

The photon detectors are two EMI 9642/2 eighteen-stage CuBe Venetian blind electron multipliers. To prevent metastable helium atoms (2^3S_1 and 2^1S_0) as well as metastable background and target gas atoms or molecules from reaching the multipliers, their view of the storage volume is covered by aluminum foils 18 mm in diameter and 800 Å thick. The foils have a transmission varying between 10% and 70% over the region 200 to 700 Å. The Al -foil, CuBe-multiplier combination responds to ≃ 2% of the radiation over the range 300 to 500 Å which strikes the Al foil. The two light pipes are Pyrex tubes coated internally with a 1000 Å thickness of gold; they enhance the count rate by about a factor of 4 over the case with no light pipes.

To establish that the observed decay is that from $He^+(2S)$ microwave power (≃150 mW) at the Lamb-shift frequency (14.045 GHz) is broadcast into the trap volume via a wave-guide horn. This converts a large fraction (more than 80%) of the 2S ions to the $2P_{1/2}$ state from which they immediately decay, destroying the 2S decay curve. The microwave power is generated by a Varian X-12 klystron and may be on-off modulated via a pin-diode switch under control of the data collection logic system.

One typical data cycle consists of the following sequence: a 0.75 msec fill period during which the electron pulse is on, a delay period of 0.8 msec during which the microwave power may or may not be applied, a storage period of 4 msec during which counts from the multipliers are accumulated versus time in 100 channels of the memory unit, and a 75 μsec ion dump period. Data are stored in two separate 100 channel blocks of the memory unit corresponding to the microwave power being on or off during the delay period. Usually the microwave power is switched on or off every 5000 data cycles. The time base for the system is derived from a 100-kHz crystal oscillator.

The pressure, p, was measured by a nude Bayard-Alpert ionization gauge calibrated against a Datametrics model 1023 capacitance manometer. For most of the targets, p ranged from zero to $\simeq 3.0 \times 10^{-6}$ Torr. The highest sensitivity of the capacitance manometer is 10^{-4} Torr full scale, thus the ion gauge was calibrated at pressures $\simeq 10$ times those used in taking the de-excitation data; this procedure is valid due to the highly linear response of the ion gauge and the fact that one requires only the slope of the ion gauge response versus absolute pressure. Put another way, to measure **R** one need only determine $\Delta(1/\tau)/\Delta n$ which in turn requires only measurement of absolute pressure increments Δp. Typical calibrations would consist of setting p to ten different values ranging from 1.0 to 10.0×10^{-5} Torr as read by the ion gauge and noting the corresponding capacitance manometer readings. The data was fit by the method of least squares to the straight line form,

$$p = M\, p_I + C, \tag{4}$$

where p_I is the ion gauge reading and M and C were varied to make the fit. For each determination of R, requiring about one day's data collection, there were made at least one and often two calibrations of the ion gauge. We found that generally the calibration constant M remained unchanged from day to day to within a few per cent and that the statistical error of the fitted M for a given set of calibration data was usually much less than 5%.

Figure 2 shows decay data for $He^+(2S)$ at three different He gas pressures. This data was used to determine R_{He}. The data are the difference between counts accumulated with microwave power on and off. Each point is the sum of three 40 μsec channels. About one hour data collection time was required to obtain each curve. The lines through the data are least squares computer fits to the function $Ae^{-t/\tau} + B$, where A, B, and τ are varied to make the fit. The constant background term B was always consistent with zero. Similar sets of curves were obtained for each of the target gases studied, although the pressure range for most was ≈ 10 times less due to the drop off of the number of stored He ions with increasing p as mentioned previously.

Figures 3, 4, and 5 show $1/\tau$ vs p data representative of that used to determine R values for all of the targets studied. Several such curves were obtained for each target and the results were determined from an average of the slopes measured by computer fit to the data.

III. Results

Table 1 contains the results of our measurements. The errors are the larger of one standard deviation of the mean of each set of measurements for a given target or 10% of the mean. In addition to the values of R we have included the ratios R/R_{He}. This quantity is equal to the ratio σ/σ_{He} if the cross sections have the same dependence on relative velocity and the relative velocity distribution is the same for both targets. The latter is a good approximation since the mean energy of the stored He^+ ions is about one half the ion trap well depth, i.e. ≃ .44 eV, whereas the mean energy of the targets is 300°K thermal, ≃ .025 eV. One can then regard the distribution of relative velocities to be essentially equal to the distribution of He^+ ion velocities which was the same for all the measurements. The greatest error would occur for the case of H_2 where the correction would increase the mean relative velocity by about 3%. One does not expect, however, that the cross sections have the same velocity dependences except among the group including the noble gases and CCl_4.

We have also included in Table 1 effective cross sections, σ_{eff}, obtained from R by dividing by the velocity $v = 4.6 \times 10^5$ cm/sec equivalent to a He ion of .44 eV energy. These are intended only to indicate the range and size of the de-excitation cross-sections for $He^+(2S)$ at this energy.

An essentially exponential decay of ground state He^+ ions versus storage time was noted during these measurements; its decay time

varied linearly with pressure p and hence is consistent with the existence of some single collision loss mechanism. In the case of noble gas targets the rate constant for this process was always quite small; $\leq 5\%$ of R. We hypothesize that possibly due to the departure of the trap geometry from a perfect quadrupole shape, certain regions of phase space can lead to ion loss. Such a loss mechanism would be proportional to the ion-atom momentum transfer cross-section and could conceivably explain the effect.

In the case of molecular targets the loss rate of ground state He^+ ions was observed to be considerably larger. In particular N_2, O_2 and CO_2 were studied. We observed loss rate constants of 1.4(3), 1.1(3), and 1.5(4) in units of 10^{-9} cm^3 sec^{-1} respectively for these targets. The rates for N_2 and O_2 are in agreement with reaction rates measured by Ferguson et al[13] and Sayers and Smith[14] for the processes,

$$He^+ + N_2 \rightarrow He + N^+ + N + .3 \text{ eV} ,$$

and

$$He^+ + O_2 \rightarrow He + O^+ + O + 5.9 \text{ eV} .$$

These authors studied the above reactions in He afterglows. Any reactions similar to the above and involving $He^+(2S)$ ions would of course be included in the measured values of R. We assume that the small loss rate mechanism ($\leq 5\%$ of R) noted for ground state ions on noble gases if present for $He^+(2S)$ collisions with these and other targets is no larger and the quoted values of R contain no correction for it.

We point out that for a perfect trap geometry one might expect some ion loss due to elastic collisions which allow a "random walk" of the ion orbit across the magnetic field or leakage along the trap axis. The latter collisions would be most probable while the ion is at one extreme of its z trajectory. Both of these processes would require multiple collisions on the average to cause loss of an ion because of the cross sectional size of the orbit ($\simeq$ 5 cm) in comparison to the trap diameter, and the small energy transfer available ($\simeq$ .025 eV) per collision. A multiple collision loss process would imply a non-exponential decay curve if it were present to any significant degree as well as a non-linear relationship between any fitted $1/\tau$ and p. Neither of these appear in our data to well within the limits indicated by the quoted errors.

In addition to measuring R values as described above, we did some experiments to determine whether or not the collision induced Lyman-alpha decay is a prominent decay mechanism for collisions with helium atoms. This was done by studying the variation of the normalized metastable decay rate, at a fixed time after creation of the ions, versus helium pressure.

The differential equation for decay of the $He^+(2S)$ population N may be rewritten as,

$$dN/dt = S_r + S_{nr} , \qquad (5)$$

where S_r and S_{nr} are rates for radiative and non-radiative processes respectively. For the case of impact on helium atoms one has,

$$S_r = -N(A+\sigma_r vn) \qquad (6)$$

$$S_{nr} = -N\sigma_{nr} vn \qquad (7)$$

where A is the free ion decay rate, $n = n_{He}$, and σ_r and σ_{nr} are cross sections for radiative and non-radiative de-excitation. The normalized

rate of photon emission, $G = S_r/N(t=0)$, at time t after creation of 2S ions at t=0 is given by,

$$G = (A+\sigma_r vn)e^{-t(A+\sigma_r vn+\sigma_{nr} vn)} \tag{8}$$

The actual measured normalized rates F, would be given by,

$$F = K(A+\xi Dp)e^{-t(A+Dp)}, \tag{9}$$

where,

$$D = (\sigma_r v+\sigma_{nr} v)/kT, \quad \text{and} \tag{10}$$

$$\xi = \eta\sigma_r v/(\sigma_r v+\sigma_{nr} v). \tag{11}$$

K is a proportionality constant involving detector geometry and efficiency factors, $p = p_{He}$ and η is the relative efficiency of the detectors for collision induced versus free decay photons. η is most probably not unity since each free decay produces two photons with a continuous single photon spectrum whereas collision produced photons are produced one/decay and are at the Lyman-α wavelength 304Å. The quantity ξ, if η=1.0, is a measure of the fraction of de-excitation collisions which produce a photon. In the above the products $\sigma_r v$ and $\sigma_{nr} v$ may be replaced by velocity averaged products.

We have measured F versus p at t=1 msec in an attempt to learn something about the size of ξ. Figure 6 shows a plot of the data. The two curves are F vs p for ξ = 0.0 and ξ= 1.0 using the measured value of $D = R_{He}/kT$, T = 300°K, and adjusting K by eye to give the best fit for ξ = 1.0. The data is consistent with $.5 \lesssim \xi \lesssim 1.5$. It is reasonable to assume that $0<\eta\lesssim 2$. Thus for collisions of $He^+(2S)$ on helium atoms we conclude that at least 25% of the de-excitation collisions produce photons.

IV. Discussion

In the following we discuss our results primarily in terms of the mechanism of induced Lyman-α decay. This is done because it is most probably the predominant de-excitation mode and to some extent one can apply the theory already developed for H(2S) de-excitation to the $He^+(2S)$ collisions studied here.

Spherical Targets

If one takes as the interaction potential between the $He^+(2S)$ ion and a target with polarizability α the form,[15]

$$U(r) = -e\alpha^2/2r^4 \tag{12}$$

with r the internuclear separation and e the electronic charge, then a simple dimensional argument shows that the induced Lyman-α decay rate should be given by

$$R = C(\alpha\mu v)^{1/2} \tag{13}$$

where C is a constant of proportionality and μ is the matrix element $|\langle 2P|z_e|2S\rangle|$, z_e being the z coordinate of the He^+ electron. (The "natural" z-axis is along the inter-nuclear axis.) We have calculated R using the potential above and straight line trajectories using the sudden approximation.[16] The sudden approximation is applicable because of the short duration of the collision, $\simeq 10^{-13}$ sec, in comparison to the 2S - $2P_{1/2}$, $2P_{3/2}$ fine structure periods, $\simeq 10^{-10}$, $\simeq 10^{-11}$ sec. The small impact parameter cut off is the usual one, i.e. that value B_0 such that $P(B_0)$ (the probability of the ion being in one of the 2P states after collision) is equal to one. The cross section is then

$$\sigma = \pi B_0^2 + 2\pi\int_{B_0}^{\infty} bP(b)db \tag{14}$$

The result of the calculation is

$$R = 6.84(e^2\alpha\mu v/\hbar)^{1/2} \tag{15}$$

For He^+, $\mu = 1.5\ a_0$, where a_0 = the Bohr radius.

Figure 7 shows a plot of the measured values of R versus $\alpha^{1/2}$ for the targets He, Ar, Kr, Xe, and CCl_4. (CCl_4 is essentially spherical; its lowest order multipole moment is the octupole.) Values of α were taken from Rothe and Bernstein.[17] One sees that the values fall well along a straight line, however they are about 50% below the sudden approximation calculation. (We used $v = 4.6 \times 10^5$ cm/sec in the calculation.) In view of the extreme over simplification of the calculation we regard the discrepancy as insignificant. We point out that any $He^+(2S)$ loss mechanism proportional to the momentum transfer cross section would also be proportional to $\alpha^{1/2}$. In the figure we include values of $\sigma_d v$ where σ_d is the momentum transfer cross section calculated from the formula of Eliason and Hirschfelder;[18]

$$\sigma_d = .553(4\pi e/v)\cdot(\alpha/M)^{1/2} \qquad (16)$$

where M is the reduced mass of the collision pair. The line through the experimental points is a least squares fit of $R = k\alpha^{1/2}$ which gave $k = 4.14 \times 10^3\ cm^{3/2}\ sec^{-1}$.

Kocher, Clendenin, and Novick[19] in their time-of-flight work on the free life-time of $He^+(2S)$ report a value of $\sigma \simeq 10\pi a_0^2 = 8.8 \times 10^{16} cm^2$ for the total de-excitation cross section of 15 eV ions on helium. This corresponds to a rate of $\simeq 2.4 \times 10^{-9}\ cm^3 sec^{-1}$. A $v^{1/2}$ scaling of our result would predict $R = 4.0 \times 10^{-9}\ cm^3 sec^{-1}$ at 15 eV.

Lipworth and Novick in reporting[20] their measurement of the He^+ $2S - 2P_{1/2}$ fine structure (Lamb shift) give the results of calculations of the cross sections, σ_r, for induced Lyman-α decay and, σ_i, for Penning ionization of He by $He^+(2S)$ ions with a mean velocity of 1.05×10^5 cm/sec. Their values are $\sigma_r = 34.4\pi a_0^2 = 3.03 \times 10^{-15} cm^2$ and $\sigma_i = 15.9\pi a_0^2 = 1.40 \times 10^{-15}$ cm^2, yielding a total cross section of $4.43 \times 10^{-15} = 44.3$ Å^2. This is quite close to the value of σ_{eff} listed in Table I for He although our estimated relative velocity is more than 4 times the value used by Lipworth and Novick in their calculation.

Linear Symmetric Molecules

In the case of impact on molecules one expects both the polarization and the molecular multipole fields to contribute to the Lyman-α de-excitation rate. For the linear symmetric molecules H_2, N_2, O_2, and CO_2 the lowest order non-vanishing multipole moment is the quadrupole. Thus one would expect that the transient electric field mixing the 2S and 2P states would be the sum of that due to the polarization of the target and its quadrupole field as a first approximation. The polarization field will in general be the sum of two dipole fields arising from induced moments $e\alpha_{\parallel}\cos\theta/r^2$ and $e\alpha_{\perp}\sin\theta/r^2$ where θ is the angle between the molecular axis and the line between the collision partners; $\alpha_{\parallel}$ and $\alpha_{\perp}$ are the polarizabilities for fields oriented parallel and perpendicular to the molecular axis. A calculation, then, requires the net electric field averaged over all molecular orientations. We do not carry out such a program here but have calculated the polarization and quadrupole field de-excitation rates as if they were acting separately. Because the two fields are not everywhere parallel,

the net effect is not simply the sum of the two, but should lie between the sum and the absolute value of the difference. The polarization field de-excitation rate, R_p, was calculated using the constant determined from the measurements on the spherical targets together with the mean polarizabilities $\bar{\alpha} = (2\alpha_\perp + \alpha_\parallel)/3$. The quadrupole field de-excitation rate was calculated using the relation $R_q = \sigma_q v$ ($v = 4.6 \times 10^5$ cm/sec), and

$$\sigma_q = 4.206(e\mu q/\hbar v)^{2/3} \tag{17}$$

from the work of Slocomb, Miller, and Schaeffer (SMS); q is the molecular quadrupole moment. The values used for q are those recommended by Stogryn and Stogryn.[21] Table 2 contains the results of these calculations. The conclusions one can draw from these results are limited. However, one sees that the sizes of the two effects are comparable; it is probably accidental that the polarization rate is in agreement with the experimental rates for H_2 and N_2 and nearly so for O_2. The case of CO_2 more clearly requires the existence of both mechanisms.

Kocher, Clendenin, and Novick[19] have also reported a value of $\sigma = 50\pi a_0^2 = 4.40 \times 10^{-15}$ cm^2 for the total de-excitation cross section for 15 eV $He^+(2S)$ on N_2. This corresponds to a rate of 11.8×10^{-9} cm^3 sec^{-1}.

Water and Ammonia

The theoretical treatment of these collisions would follow the discussion in the previous section with the addition of the electric dipole fields arising from the large dipole moments of these molecules

(1.84 and 1.47 × 10^{-18} esu cm for water and ammonia[21]). Using mean polarizabilities[17] of 1.45 and 2.16 × 10^{-24} cm^{-3} for water and ammonia one obtains 5.0 and 6.1 × 10^{-9} cm^3 sec^{-1} for the de-excitation rates due to the polarization field alone.

The electric dipole fields alone would yield, for water, 39.6 × 10^{-9} and for ammonia, 31.5 × 10^{-9} cm^3 sec^{-1} using the method of SMS; the results of Gersten's method are larger by a factor of $3^{1/2}$.

An effective quadrupole moment of 1.0 × 10^{-26} esu cm^2 (appropriate for both molecules) would yield a rate of 3.5 × 10^{-9} cm^3 sec^{-1} using the method of SMS and a factor of $3^{1/3}$ larger from the work of Gersten.

Calculations of the octupole components of the water molecule yield values ≃ 10^{-34} esu cm^3 which would imply a rate, if acting alone of .60 × 10^{-9} cm^3 sec^{-1}. In all of the above a relative velocity of 4.6 × 10^5 cm/sec has been assumed.

The experimental values of the total de-excitation rate (Table I) for water and ammonia are considerably less (about 50%) than the rates calculated for the permanent dipole fields and listed above. This may reflect partial cancellation of the dipole field by the induced dipole and higher order multipole fields. In any case the measured values await a complete calculation of the Lyman-α de-excitation rates for impact of $He^+(2S)$ on these molecules before a more meaningful comparison can be made.

References

† Work supported by the U.S. Atomic Energy Commission.

[1] R. S. Kass and W. L. Williams, Phys. Rev. A7, 10 (1973).

[2] S. J. Czuchlewski and S. R. Ryan, Bull. Am. Phys. Soc. 17, 1136 (1972); Bull. Am. Phys. Soc. 18, 687 (1973); S. J. Czuchlewski, Ph.D. Thesis (Yale University 1973).

[3] F. J. Comes and U. Wenning, Z. Naturforsch, 24a, 587 (1969); Chem. Phys. Letters 5, 199 (1970).

[4] W. L. Fite, R. T. Brackmann, D. G. Hummer, and R. F. Stebbings, Phys. Rev. 116, 363 (1959); Phys. Rev. 124, 2051 (1961).

[5] W. L. Fite, W. E. Kauppila, and W. R. Ott, Phys. Rev. Letters 20, 409 (1968); W. R. Ott, W. E. Kauppila, and W. L. Fite, Phys. Rev. A1, 1089 (1970).

[6] F. W. Byron, Jr. and J. I. Gersten, Phys. Rev. A3, 620 (1971); Phys. Rev. Letters 30, 115 (1973).

[7] J. I. Gersten, J. Chem. Phys. 51, 637 (1969).

[8] C. A. Slocomb, W. H. Miller and H. F. Schaefer III, J. Chem. Phys. 55, 926 (1971).

[9] M. H. Prior, Phys. Rev. Letters, 29, 611 (1972).

[10] J. Shapiro and G. Breit, Phys. Rev. 113, 179 (1959); S. Klarsfeld, Phys. Letters 30A, 382 (1969).

[11] H. A. Bethe and E. E. Salpeter, Quantum Mechanics of One- and Two-Electron Atoms (Academic, New York, 1957), Chap.4, p.285.

[12] L. Spitzer and J. L. Greenstein, Astrophys. J. 114, 407 (1951).

[13] E. E. Ferguson, F. C. Fehsenfeld, D. B. Dunkin, A. L. Schmeltekopf, and H. I. Schiff, Planet Space Sci. 12, 1169 (1964).

[14] J. Sayers and D. Smith in Atomic Collision Processes, edited by M. R. C. McDowell (North-Holland, Amsterdam, 1964), p. 871.

[15] J. B. Hasted, Physics of Atomic Collisions (Butterworths, London, 1964), Chap. 2, p. 35.

[16] L. I. Schiff, Quantum Mechanics 3rd Edition (McGraw-Hill, New York, 1968), Chap. 8, p. 292.

[17] E. W. Rothe and R. B. Bernstein, J. Chem. Phys. 31, 1619 (1959).

[18] M. A. Eliason and J. O. Hirschfelder, J. Chem. Phys. 30, 1426 (1959); M. A. Eliason, D. E. Stogryn, and J. O. Hirschfelder, Prox. Natl. Acad. Sci. U. S. 42, 546 (1956).

[19] C. A. Kocher, J. E. Clendenin, and R. Novick, Phys. Rev. Letters 29, 615 (1972).

[20] E. Lipworth and R. Novick, Phys. Rev. 108, 1434 (1957).

[21] D. E. Stogryn and A. P. Stogryn, Mol. Phys. 11, 371 (1966).

TABLE I. Results of $He^+(2S)$ de-excitation rate measurements.

Target	R ($10^{-9}cm^3sec^{-1}$)	R/R_{HE}	σ_{eff} [a] ($Å^2$)
He	1.65(17)	1.00	37.
Ar	4.99(65)	3.02(50)	112.
Kr	6.3(10)	3.82(72)	143.
Xe	8.7(14)	5.24(55)	196
CCl_4	13.3(13)	8.1(12)	302.
H_2	3.68(37)	2.23(32)	83.
N_2	5.51(55)	3.34(48)	125.
O_2	6.07(61)	3.68(53)	137.
CO_2	11.3(16)	6.9(12)	258.
H_2O	18.5(19)	11.2(16)	420.
NH_3	20.9(21)	12.6(18)	473.

[a] $\sigma_{eff} = R/v$, $v = 4.6 \times 10^5 cm/sec$

TABLE II. Comparison of experimental de-excitation rates, R, with polarization, R_p, and quadrupole, R_q, rates. $\bar{\alpha}$ and q are the mean polarizability and quadrupole moment used in calculating R_p and R_q.

Target	$\bar{\alpha}$ [a] ($Å^3$)	q [b] (10^{-26}esu cm^2)	(10^{-9} cm^3 sec^{-1})		
			R [c]	R_p	R_q [d]
H_2	0.806	0.651	3.68(37)	3.72	2.65
N_2	1.74	-1.52	5.51(55)	5.46	4.66
O_2	1.57	-0.39	6.07(61)	5.19	1.88
CO_2	2.59	-4.3	11.3(16)	6.67	9.32

[a]Ref.17 [b]Ref.21 [c]See Table I. [d]Using method of SMS(Ref.8)

Figure Captions

Fig. 1. Sketch of the ion trap and photon detectors. The magnetic field is along the trap axis. The half cylinders 2a and 2b are maintained negative with respect to electrodes 1 and 3 during the storage period. The hot filament F is pulsed negative to accelerate electrons into the trap for creation of the He ions. The zig-zag pattern is a web of thin copper wires to give high transparency for the decay photons, while maintaining the cylindrical electrode geometry. The rectangular shape in the center of the figure represents the end of the microwave horn located outside the cylinder. Power radiated from this horn drives the $2S\text{-}2P_{1/2}$ transition.

Fig. 2. Representative $He^+(2S)$ decay curves for three different pressures of He. The lines are computer fits. The curves have been adjusted slightly vertically so that the lines meet at t=0. The ordinate is correctly scaled for the data at 7.0×10^{-6} Torr.

Fig. 3. $^1/_\tau$ vs pressure plots for $He^+(2S)$ collisions with H_2 and He. The lines are least squares computer fits.

Fig. 4. $^1/_\tau$ vs pressure plots for $He^+(2S)$ collisions with He, Ar, Kr, Xe, and CCl_4. The curves have been separated vertically for clarity since the slopes are the quantities of interest. The lines are least squares computer fits. The line for He is that shown in Fig. 3.

Fig. 5. $^1/_\tau$ vs pressure plots for $He^+(2S)$ collisions with H_2, N_2, O_2, CO_2, H_2O, and NH_3. The curves have been separated vertically for clarity since the slopes are the quantities of interest. The lines are least squares computer fits. The line and points for H_2 are the low pressure end of the plot shown in Fig. 3.

Fig. 6. Plot of the normalized count rate for $He^+(2S)$ in collision with He at t = 1 msec after creation of the ions versus He pressure. The upper and lower curves are plots of the function F for $\xi = 1.0$ and 0.0, respectively. The data indicates that at least 25% of the collisions produce countable photons.

Fig. 7. Plot of experimental values of the $He^+(2S)$ total de-excitation rate versus the square root of the polarizability of the targets He, Ar, Kr, Xe, and CCl_4. The dashed line is the result of a sudden approximation calculation. The triangles are momentum transfer rates for $v = 4.6 \times 10^5$ cm/sec. The solid line is a least squares straight line fit to the data.

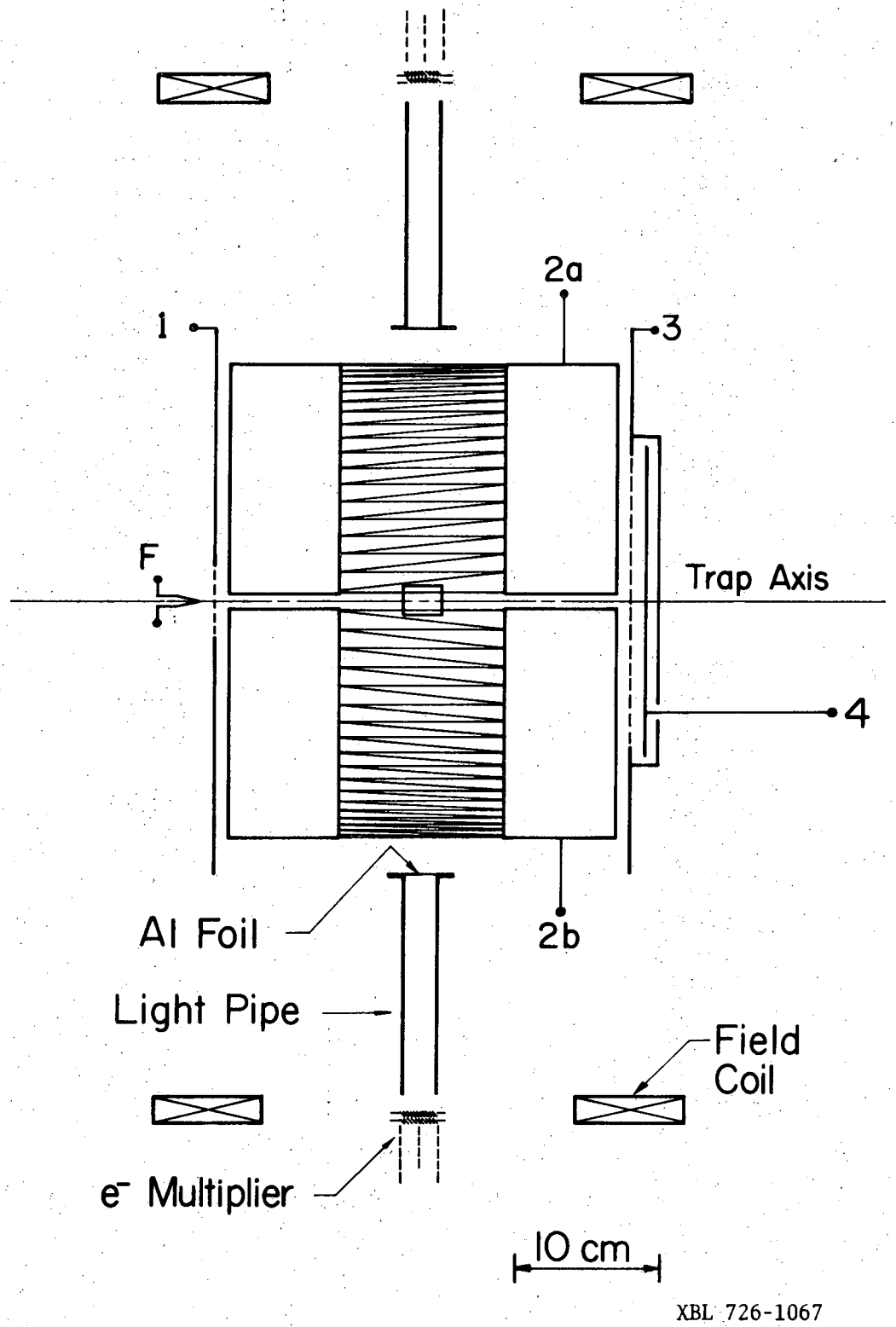
2a
1
3
F
Trap Axis
4
Al Foil
2b
Light Pipe
Field
Coil
e⁻ Multiplier
10 cm
XBL 726-1067

Fig. 1

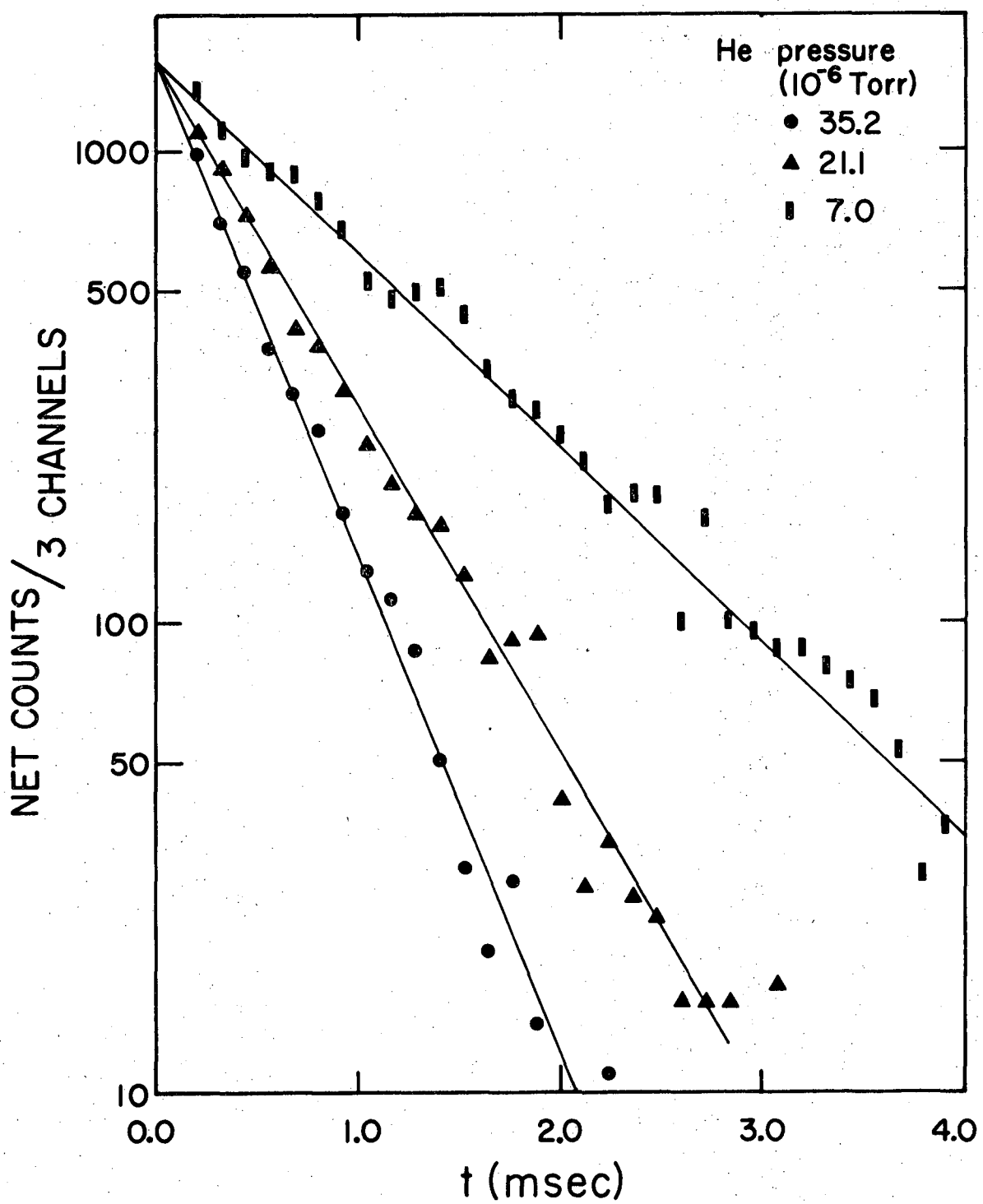

XBL 739-1237

Fig. 2

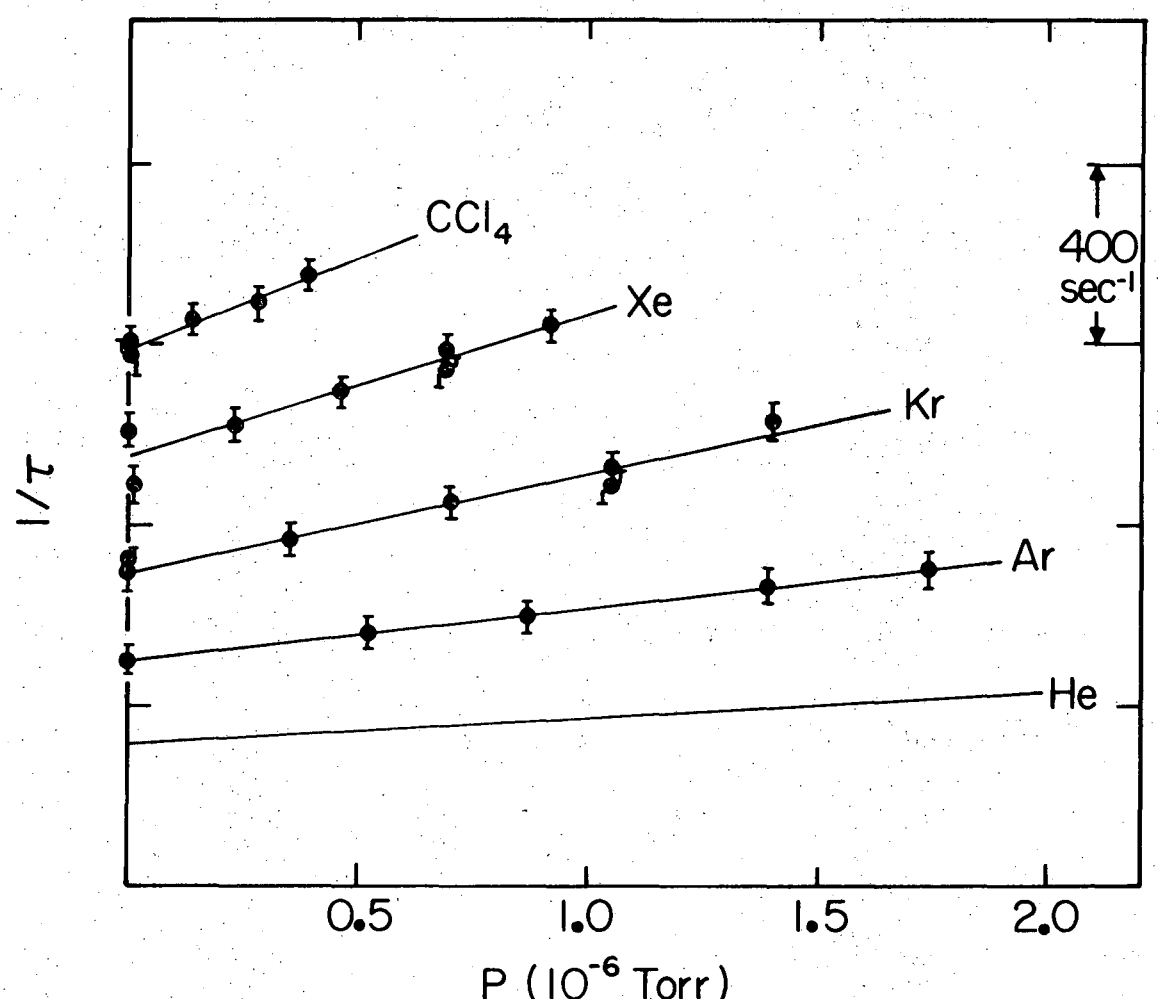

XBL 739-1232

Fig. 3

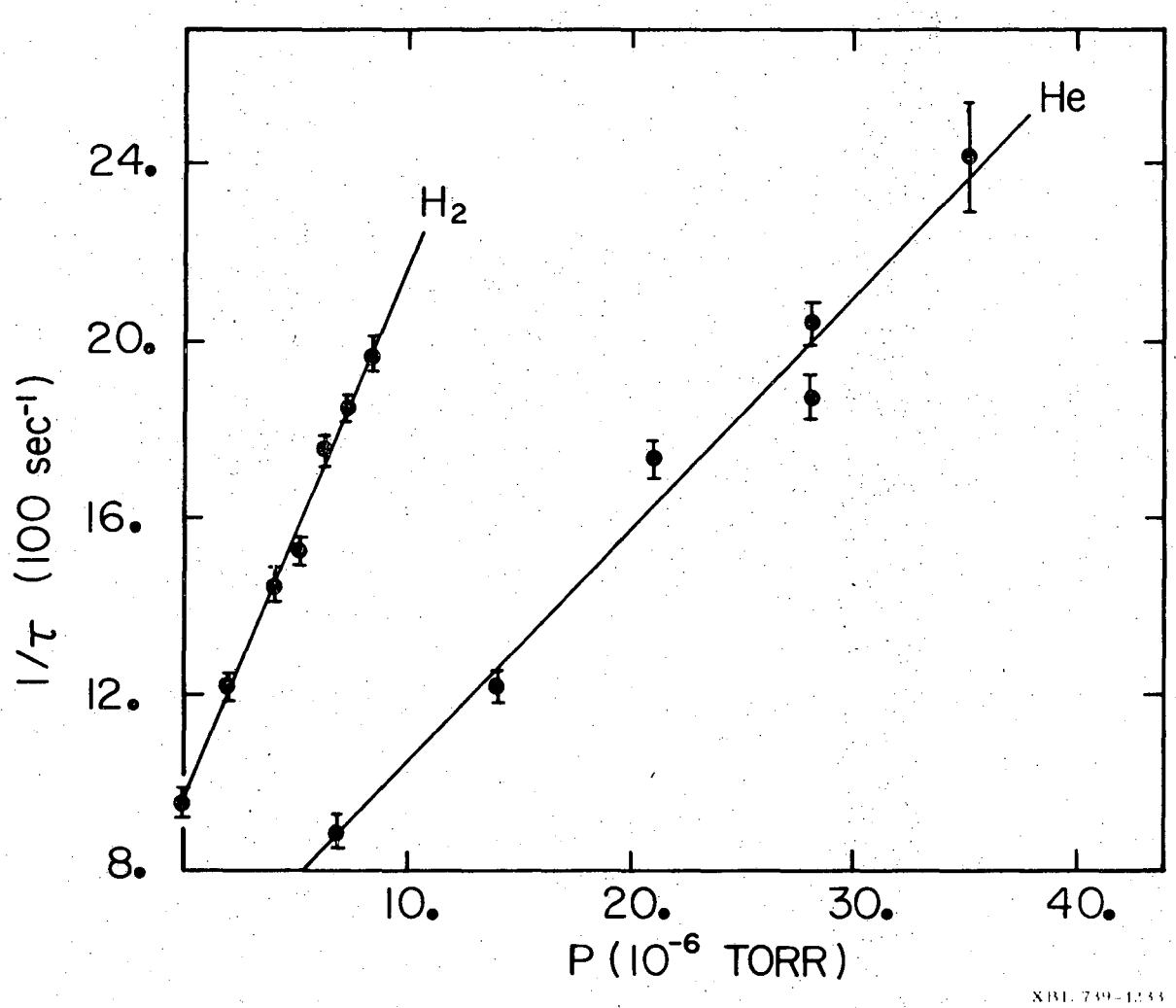
He
H_2
24.
20.
16.
12.
8.
$1/\tau$ (100 sec^{-1})
10.
20.
30.
40.
P (10^{-6} TORR)
XBL 749-1233

Fig. 4

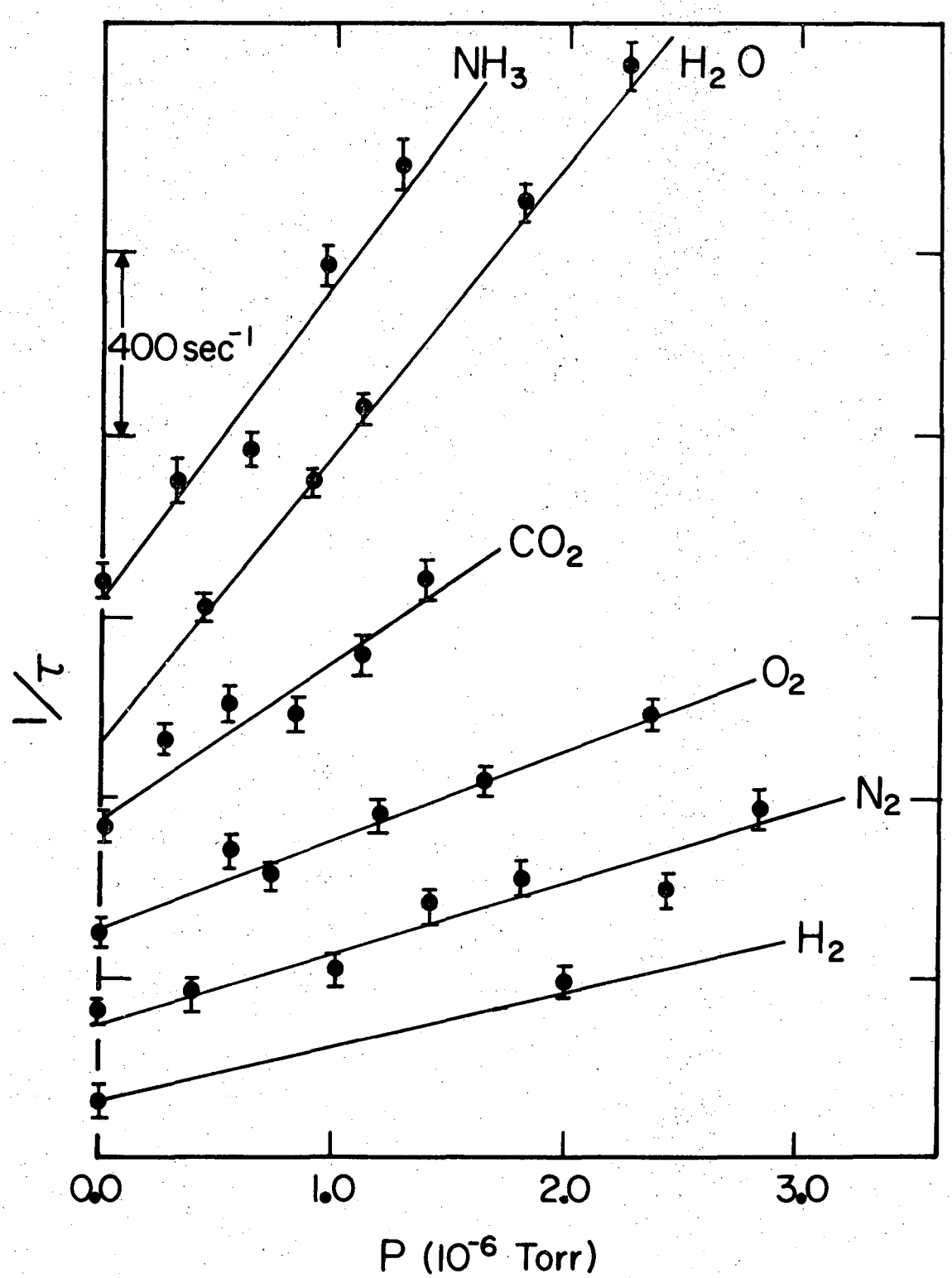

XBL 739-1235

Fig. 5

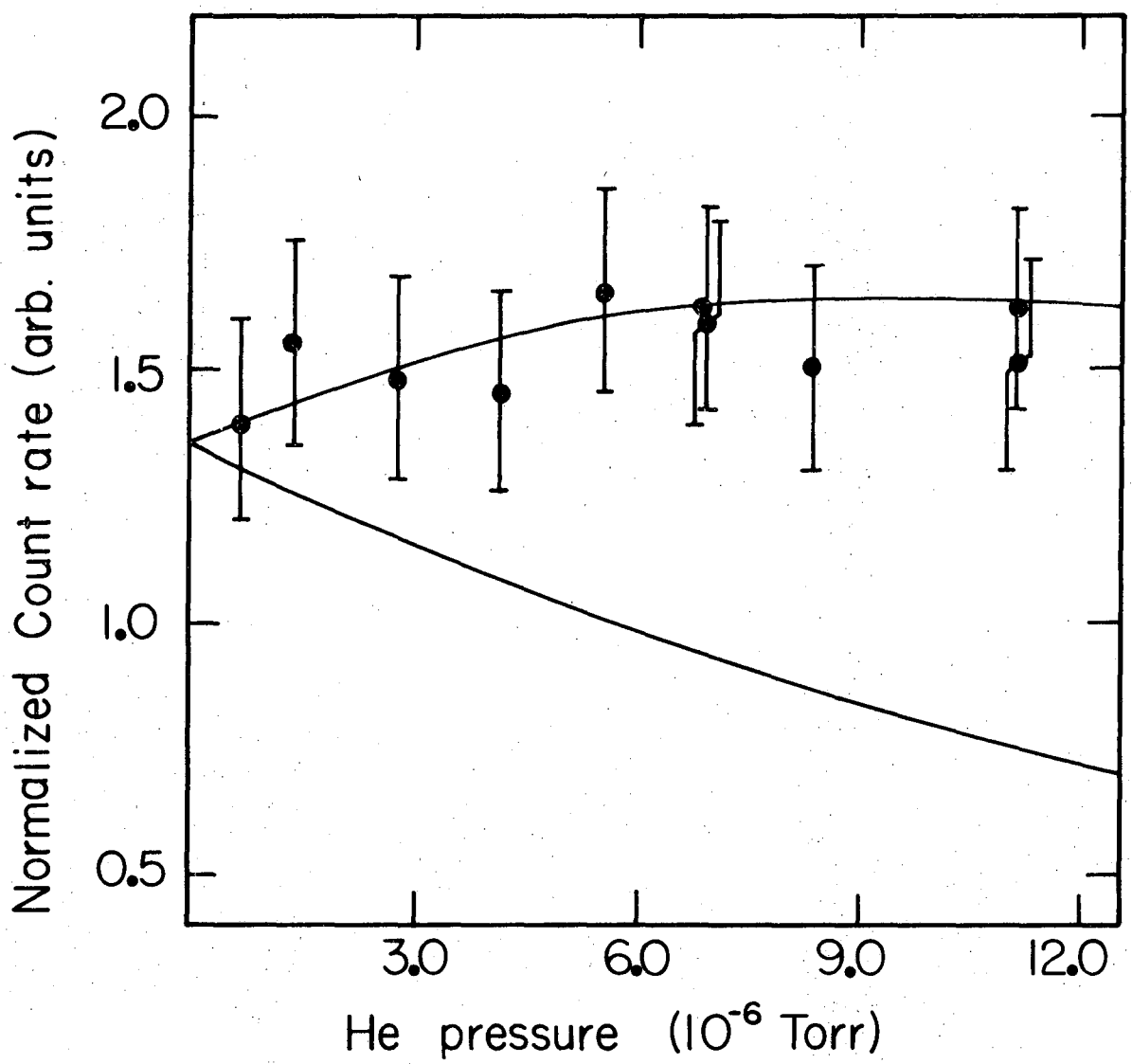

XBL 739-1236

Fig. 6

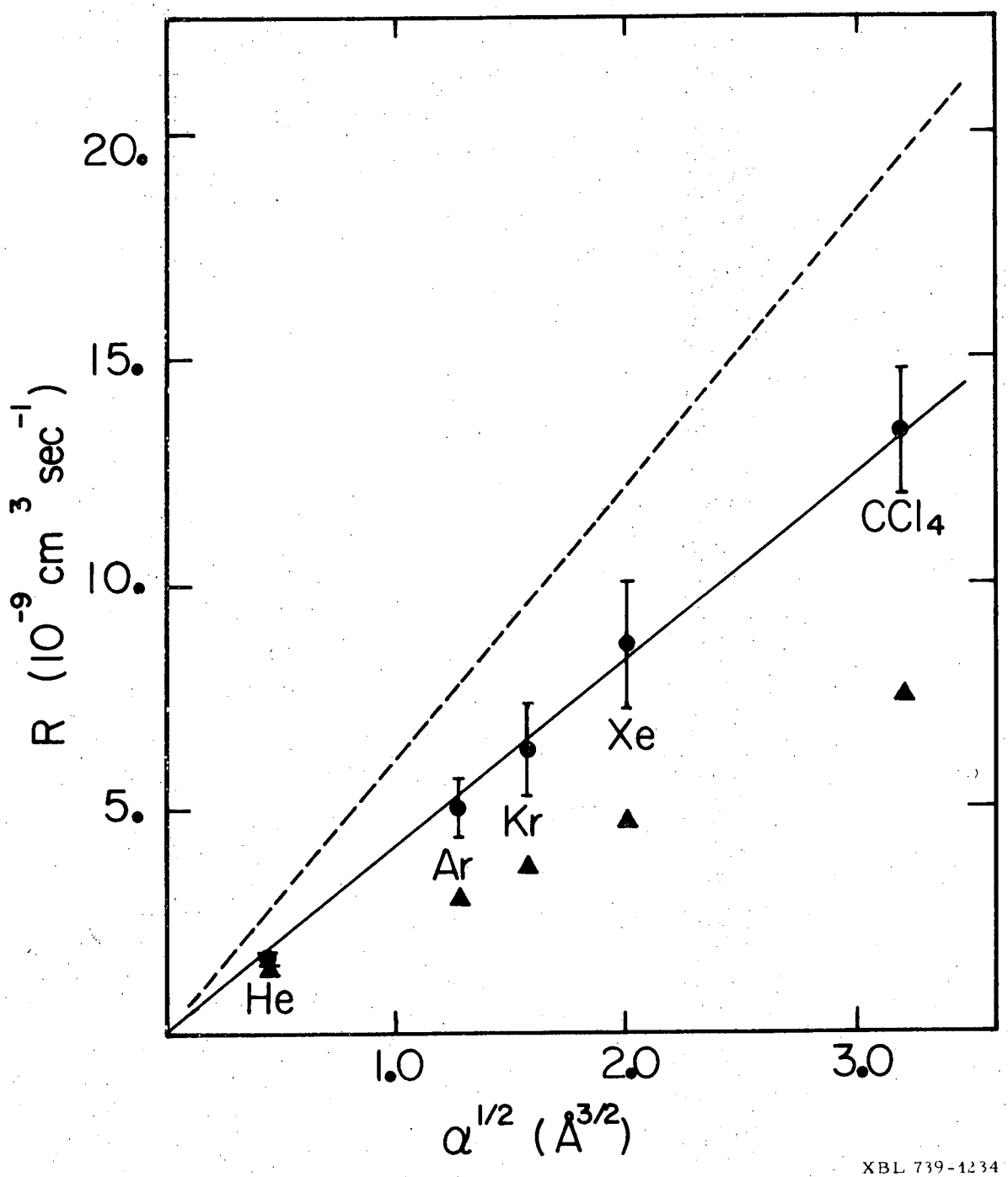

XBL 739-1234

Fig. 7

LEGAL NOTICE

This report was prepared as an account of work sponsored by the United States Government. Neither the United States nor the United States Atomic Energy Commission, nor any of their employees, nor any of their contractors, subcontractors, or their employees, makes any warranty, express or implied, or assumes any legal liability or responsibility for the accuracy, completeness or usefulness of any information, apparatus, product or process disclosed, or represents that its use would not infringe privately owned rights.

TECHNICAL INFORMATION DIVISION
LAWRENCE BERKELEY LABORATORY
UNIVERSITY OF CALIFORNIA
BERKELEY, CALIFORNIA 94720